Biochimica et Biophysica Acta 1850 (2015) 708–721

Contents lists available at ScienceDirect

Biochimica et Biophysica Acta

journal homepage: www.elsevier.com/locate/bbagen

MiR-143 and rat embryo implantation

Shi Tian [a,1], Xing Su [b,c,1], Lu Qi [b,1], Xiao-Hua Jin [b,c], Yi Hu [b], Chun-Ling Wang [d], Xu Ma [b,c,*], Hong-Fei Xia [b,c,*]

[a] Haidian Maternal & Child Health Hospital, Beijing 100080, China
[b] Reproductive and Genetic Center of National Research Institute for Family Planning, Beijing 100081, China
[c] Graduate School, Peking Union Medical College, Beijing 100730, China
[d] Cadre Ward, China Mei-Tan General Hospital, Beijing 100028, China

ARTICLE INFO

Article history:
Received 5 June 2014
Received in revised form 26 November 2014
Accepted 29 November 2014
Available online 5 December 2014

Keywords:
miR-143
Embryo implantation
Uterus
Rat
Lifr

ABSTRACT

Background: To study the role of *miR-143* during embryo implantation in rat.
Methods: MiR-143 expression in rat early pregnancy was detected by Northern blot. The relation between *miR-143* and *Lifr* predicted and confirmed by bioinformatics method, dual-luciferase activity assay, Western blot and immunohistochemistry. The role of *miR-143* was detected by MTS, Edu and *ranswell* chamber assays.
Results: The expression level of *miR-143* on gestation day 5–8 (g.d. 5–8) was higher than on g.d. 3–4 in uteri of pregnant rat. *MiR-143* was mainly localized in the superficial stroma/primary decidual zone, luminal and glandular epithelia. The expression of *miR-143* was not significantly influenced by pseudopregnancy, but the activation of delayed implantation and experimentally induced decidualization significantly promoted *miR-143* expression. Over-expression of *miR-143* in human endometrial stromal cells (ESCs) inhibited cell proliferation, migration and invasion. Knockdown of *miR-143* promoted cell proliferation and invasion. The results of recombinant luciferase reporters showed that *miR-143* could bind to the 3¢-untranslated region (UTR) of *leukemia inhibitory factor receptor* (*Lifr*) to inhibit *Lifr* translation.
Conclusions: Uterine *miR-143* may be involved in the successful pregnancy, especially during the process of blastocyst implantation through regulating *Lifr*.
General significance: This study may have the potential to provide new insights into the understanding of ***miR-143*** function during embryo implantation.

1. Introduction

Mir-143 is a short non-coding RNAs molecule and located on chromosome 5 position 33 in the human genome [38]. *MiR-143* is highly conserved in vertebrates and function to regulate the expression levels of their target genes by binding to their 3′-untranslated regions (3′-UTR) [11,12,38]. *MiR-143* also down-regulates the expression levels of their target genes through targeting their coding regions [43].

MiR-143 is thought to play an important role in tumorgenesis. Decreased expression of *mir-143* has been observed in diversified cancer samples, such as bladder cancer, cervical cancer, colorectal cancer, liposarcomas, prostate carcinomas, non-small cell lung cancer, breast cancer, endometrioid carcinomas, renal cell carcinoma and so on [1,9,13,18,19,30,44–47]. Loss of *miR-143/145* cluster enhanced cancer cell migration and invasion in prostate cancer through directly regulating Golgi membrane protein 1 (GOLM1) [22]. The chemically modified *miR-143* duplex showed a significant tumor-suppressive effect on xenografted tumors of human colorectal cancer DLD-1 cells and may be a candidate for an RNA medicine for the treatment of colorectal tumors [21]. There are striking similarities present between the behavior of invasive placental cells during embryo implantation and that of invasive cancer cells [29]. Implantation of the embryo is one of the last great mysteries of reproductive biology. *MiR-143* was found to be upregulated at implantation sites in mouse uterus on day 5 of pregnancy compared with inter-implantation sites [15]. Our previous study also showed that *miR-143* was differentially expressed in rat uteri between pre-receptive and receptive phase via microRNA (miRNA) microarray analysis [40]. However, the roles of *miR-143* during embryo implantation remain unclear.

In the present study, we measure the expression and regulation of *miR-143* in uterus during peri-implantation in rat. Additionally, we analyze the effects of *miR-143* on cell viability, migration and invasion, and investigate the regulatory target of *miR-143*.

2. Materials and methods

2.1. Experimental animals and protocols

Sexually mature female Sprague Dawley rats (220–260 g body weight) were purchased from the Laboratory Animal Center of the

* Corresponding authors at: Genetic Center of National Research Institute for Family Planning, Beijing 100081, China. Tel.: +86 1 62178932; fax: +86 1 62179059.
E-mail addresses: chinawang2007@163.com (C.-L. Wang), genetic@263.net.cn (X. Ma), hongfeixia@126.com (H.-F. Xia).
[1] These two authors contributed equally to this work.

http://dx.doi.org/10.1016/j.bbagen.2014.11.023
0304-4165/

Academy of Military Medical Sciences (Beijing, China). Rats were housed in a temperature- and humidity-controlled room with a 12/12 h light/dark cycle. All animal procedures were approved by the Institutional Animals Care and Use Committee of the National Research Institute for Family Planning. Rats were caged overnight with fertile males of the same strain. The presence of a vaginal plug or sperm was

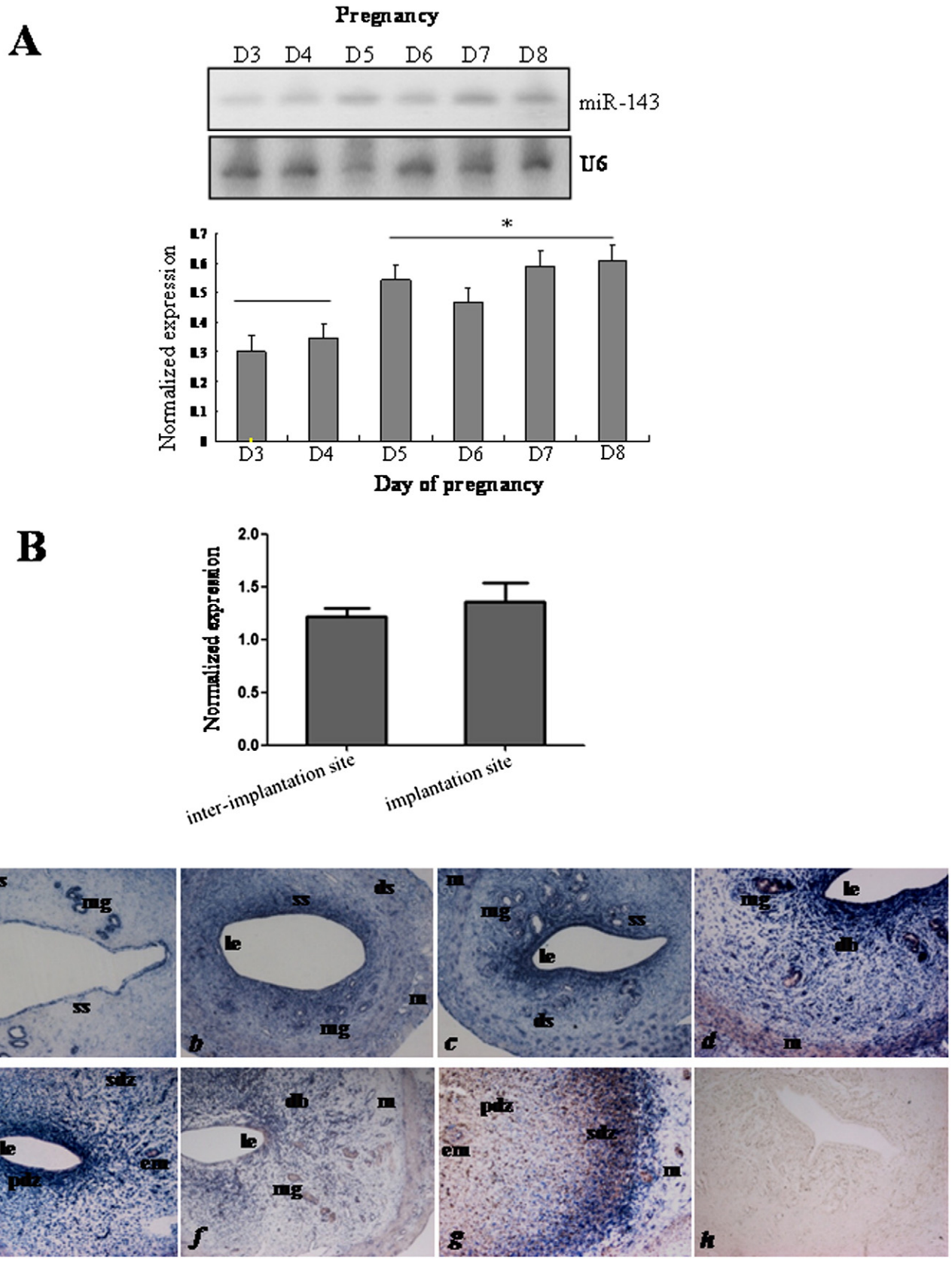

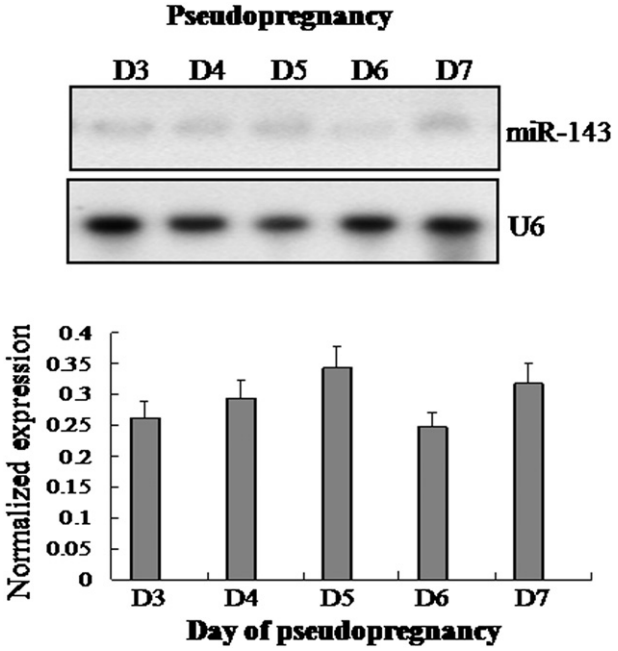

Fig. 2. The expression pattern of *miR-143* in rat uteri in the model of pseudopregnancy detected by Northern blot. $^{*}P < 0.05$, $^{**}P < 0.01$.

considered as day 1 of pregnancy (g.d. 1). The rats were euthanized at nine o'clock g.d. 3–8 morning, and uteri were excised and fixed with 4% paraformaldehyde (PFA) solution (Sigma-Aldrich, St. Louis, MO, USA) for *in situ* hybridization or frozen in liquid nitrogen for RNA analysis.

Pseudopregnancy was induced by caging adult females with vasectomized males and mating was confirmed by checking for a vaginal plug (day 1 of pseudopregnancy). The uteri were collected from day 3–7 of pseudopregnancy. On day 5 of pseudopregnancy, when the uteri were optimally sensitized for artificial deciduogenic stimuli, 100 μL olive oil (Sigma-Aldrich) was infused into the lumen of one of the uterine horns to induce artificial decidualization. The contralateral uterine horn, which was not infused with oil, served as a control. At day 7 of pseudopregnancy, the rats were euthanized and the uterine horns were isolated.

To induce delayed implantation, the pregnant rats on g.d. 4 were ovariectomized. Progesterone (P4; 5 mg/rat, s.c.; Sigma-Aldrich) was injected to maintain delayed implantation from g.d. 5 to 7. The progesterone-primed delayed-implantation rats were treated with estradiol-17β (E2; 0.5 μg/rat; Sigma-Aldrich) to terminate delayed implantation. The rats were euthanized by stunning and cervical dislocation to collect uteri at 24 h after estrogen treatment. The implantation sites were also identified by intravenous injection of Chicago blue solution (Sigma-Aldrich). To confirm that the rats receiving progesterone only were in a state of delayed implantation, uterine flushings were collected from g.d. 5 to 7 and examined for the presence of hatched blastocysts.

The female rats were ovariectomized. After 2 weeks, the ovariectomized rats were injected with E2 (1 μg/rat) or P4 (10 mg/rat) dissolved in olive oil. Control rats were administered with olive oil only (0.1 ml/rat). The uterine tissues were collected 24 h after the hormonal treatment.

2.2. Northern blot analysis

Total RNA was isolated from uterus with TRIzol reagent (Invitrogen, Carlsbad, CA, USA). Aliquots of 40 μg of total RNA per sample were subjected to electrophoresis on a 15% urea-PAGE gel and transferred to a nylon membrane (Hybond N+; Amersham Pharmacia Biotech, St Albans, Hertford, UK). After being UV cross-linked and baked at 50 °C for 30 min, the membrane was prehybridized with hybridization buffer at 42 °C for 4 h and then hybridized with ^{32}P-labeled *miR-143* probes (TGAGCTACAGTGCTTCATCTCA) and U6 probes (CGTTCCAATTTTAGTATATGTGCTGCCGAAGCGA) at 40 °C overnight. Membranes were washed and exposed to PhosphorImager screens (GE Healthcare Bio-Sciences Corp., Piscataway, NJ, USA). The bands were analyzed using Quantity One software (Bio-Rad, Hercules, CA, USA). All experiments were repeated at least three times.

3. TaqMan miRNA RT-real time PCR

Total RNA was extracted from tissues and cells, using Trizol (Invitrogen, Carlsbad, CA, USA) according to the manufacturer's instructions. Single-stranded cDNA was synthesized by using TaqMan MicroRNA Reverse Transcription Kit (Applied Biosystems, Foster City, CA, USA) and then amplified by using TaqMan Universal PCR Master Mix (Applied Biosystems) together with miRNA-specific TaqMan MGB probes: *miR-143* and *U6* according to the manufacturer's instructions (Applied Biosystems). The U6 snoRNA was used for normalization. Each sample in each group was measured in triplicate and the experiment was repeated at least three times.

3.1. In situ hybridization

Sections of uterus (5 μm) were treated with proteinase K (20 g/ml) for 15 min and refixed in 4% PFA for 15 min. After acetylation with 0.25% acetic anhydride in 0.1 M triethanolamine (pH 8.0) for 10 min, sections were prehybridized with hybridization buffer (Roche, Mannheim, Germany) at 40 °C for 2 h and then hybridized with digoxigenin (DIG)-labeled LNA-miR-143 probe (LNA-miR-143 sequence: 5′-DIG-tgAgcTacAGtGcTtCatCtca-3′) at 40 °C overnight. The sections were then incubated in buffer containing anti-DIG-antibody for 2 h at 37 °C, followed by staining with 5-bromo-4-chloro-3-indolyl phosphate (BCIP) and p-nitroblue tetrazolium chloride (NBT) (Promega, Madison, WI, USA). The sections were hybridized with a DIG-labeled LNA-scrambled probe (LNA-scrambled sequences: 5′-caTtaAtgTcGgaCaaCtcAat-3′) as a negative control. The sections were observed with an Eclipse 80i microscope (Nikon, Tokyo, Japan).

3.2. Cell viability assay

In vitro cell viability was estimated with an MTS assay. Briefly, human endometrial stromal cells (ESCs) (5000 cells/well) were seeded in 96-well plates (Corning Costar Corp., Cambridge, MA, USA) in DMEM/F12 culture, and allowed to attach overnight. The cells were then transfected with *miR-143* mimics, pre-miR control, *miR-143* inhibitor and anti-miR control, respectively. The final concentration is 50 nM. *MiR-143* mimics are chemically synthesized, double-stranded RNAs which mimic mature endogenous *miR-143* after transfection into cells. *MiR-143* inhibitor is chemically synthesized, single-stranded, modified RNAs which specifically inhibit

Fig. 1. The expression pattern of *miR-143* in rat uterus during peri-implantation period. A. The expression of *miR-143* in rat uteri from g.d. 3 to 8 was detected by Northern blot. Hybridization was conducted with a ^{32}P-labeled probe specific for *miR-143* and *U6*. *U6* snRNA was used as loading control to normalize for gel loading and transfer. The histogram represents the *miR-143* levels quantified by densitometric analysis and expressed as ratio of *miR-143* to *U6* intensity. $^{*}P < 0.05$. B. The expression of *miR-143* in the implantation sites and the inter-implantation sites of rat uteri on day 6 of pregnancy was detected by TaqMan miRNA RT-real time PCR. U6 serves as an internal reference. $^{*}P < 0.05$. C. *In situ* localization of *miR-143* in rat uteri during early pregnancy. Uteri sections from Day 3 (*a*), Day 4 (*b*), Day 5 (*c*), inter-implantation sites and implantation sites of Day 6 (*d* and *e*) and Day 7 (*f* and *g*) of pregnancy were subjected to *in situ* hybridization using DIG-labeled LNA probe specific to *miR-143*. To evaluate the specificity of the probe, negative control staining was performed using DIG-labeled LNA-scrambled probe (*h*). Blue stain indicates hybridization signals. The photographs are shown at ×100 original magnification. Key: m, myometrium; mg, maternal gland; le, luminal epithelium; ss, superficial stroma; ds, deep stroma; pdz, primary decidual zone; sdz, secondary decidual zone; s, stroma; db, decidua basalis; em, embryo.

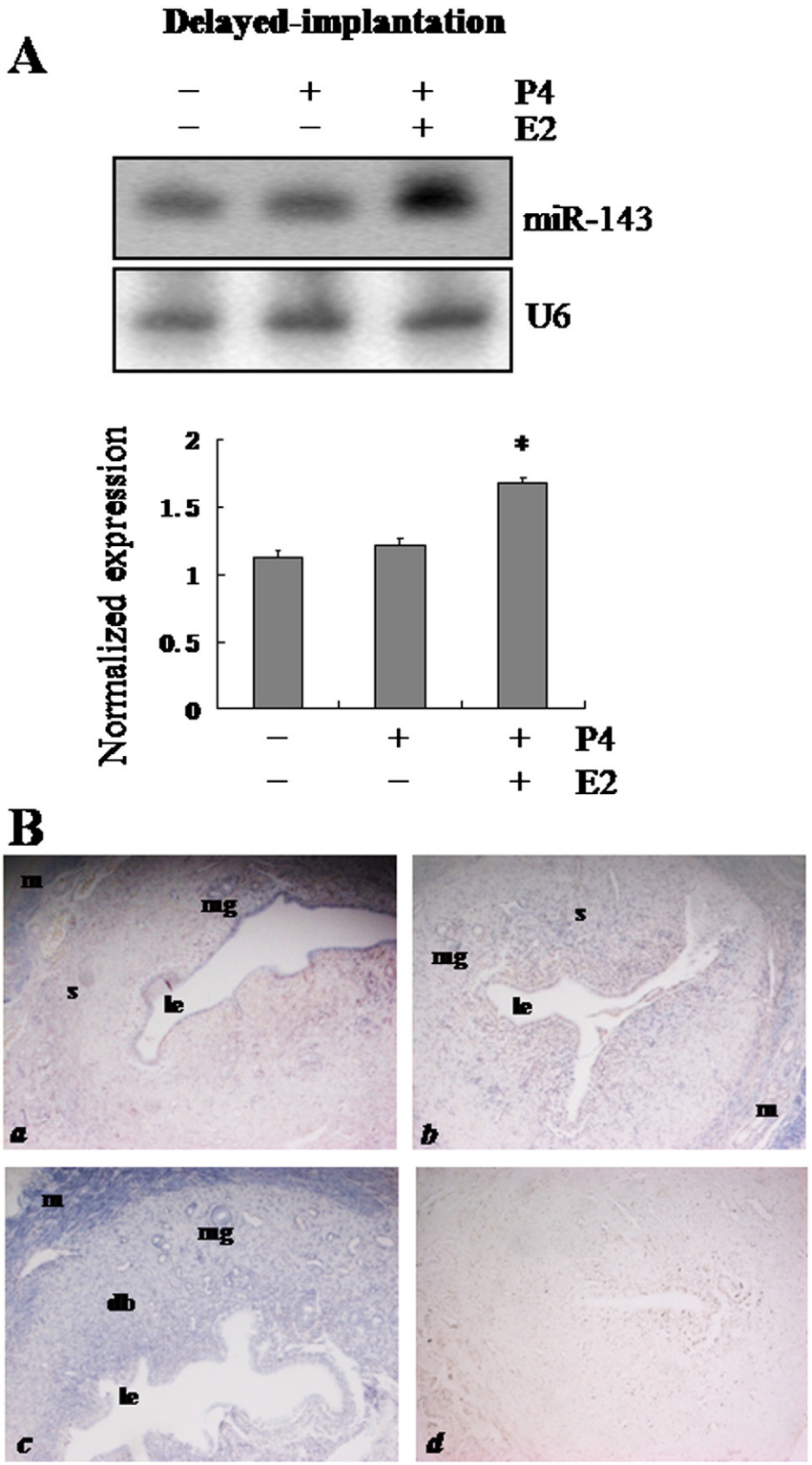

Fig. 3. The expression pattern of *miR-143* in rat uteri in the model of activation of delayed-implantation. Northern blot (A) and *in situ* hybridization (B) were used to detect the expression of *miR-143* in rat uteri of delayed-implantation (B *a* and *b*) and activation of delayed-implantation (B *c*). Blue stain indicates hybridization signals. The photographs are shown at ×100 original magnification. Key: m, myometrium; mg, maternal gland; le, luminal epithelium; s, stroma; db, decidua basalis. $^{*}P < 0.05$, $^{**}P < 0.01$.

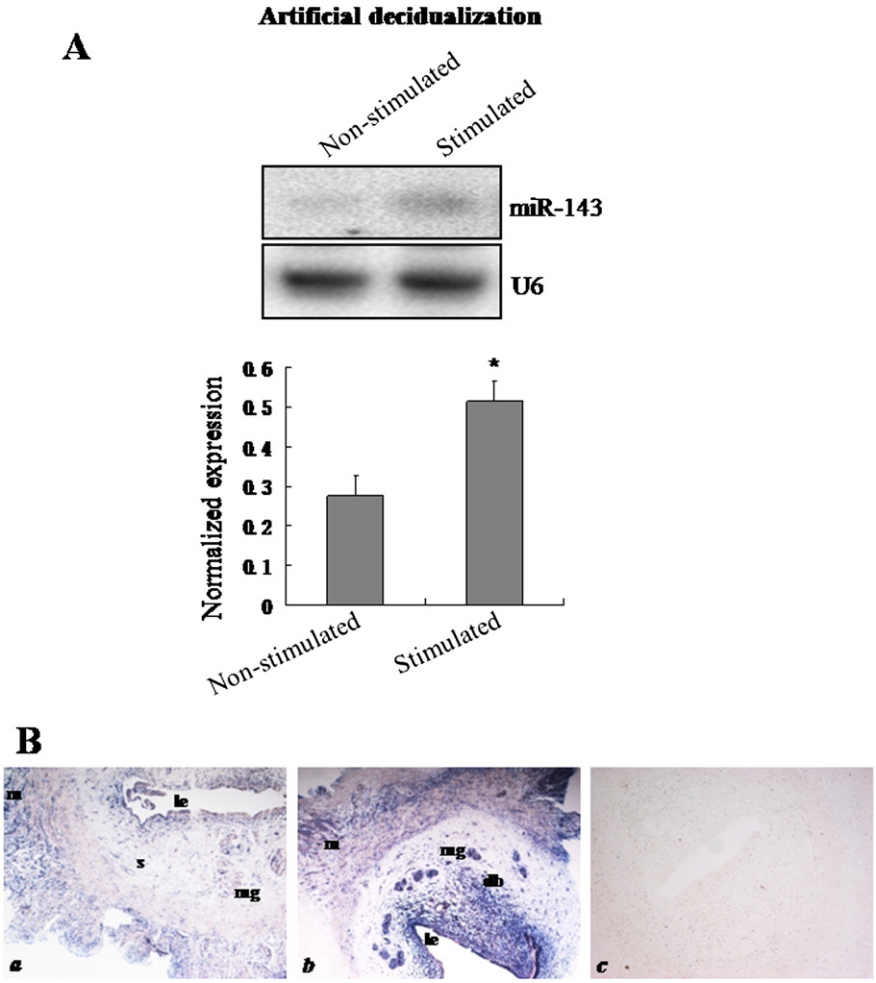

Fig. 4. The expression pattern of *miR-143* in rat uteri in the model of artifical decidualization. Northern blot (A) and *in situ* hybridization (B) were used to detect the expression of *miR-143* in the non-stimulated (B *a*) and stimulated (B *b*) uteri of artifical decidualization. Blue stain indicates hybridization signals. The photographs are shown at ×100 original magnification. Key: m, myometrium; mg, maternal gland; le, luminal epithelium; s, stroma; db, decidua basalis. $^{*}P < 0.05$, $^{**}P < 0.01$.

endogenous *miR-143* function after transfection into cells. Twenty microlitre MTT (5 mg/ml; Sigma-Aldrich) were added to each well 48 h after transfection, and the cells were incubated for 4 h. Media was then removed and the 150 μl dimethyl sulfoxide (Sigma-Aldrich) was added in each well. Absorbance was recorded at A570 nm with a 96-well plate reader (Bio-Rad 3550). The experiment has been repeated for three times.

Cell proliferation was also estimated using Cell-Light Edu Apollo DNA *in vitro* Kit (Guangzhou RiboBio Co., Ltd, Guangzhou, China). Proliferative cells were visualized and imaged using a Zeiss LSM 510 META Laser Scanning Confocal Microscopy (Carl Zeiss, Jena, Germany). Proliferative cells were counted in different optical fields (magnification ×100) selected in a random manner and analyzed by the software of AxioVision Rel. 4.8 (Carl Zeiss).

3.3. In vitro migration and invasion assays

ESCs were infected with the *miR-143* mimics, pre-miR control, *miR-143* inhibitor or anti-miR control, respectively. The infected cells were harvested and subjected to the following assays, 48 h after transfection. For migration assays, the infected cells (0.5×10^6 cells/ml) were seeded in the top of an 8.0-μm-pore membrane chamber (Corning Costar Corp.). Following a 17 h incubation period, cells that passed through the membrane to attach to the bottom of membrane were fixed and stained with hematoxylin and eosin (Sigma-Aldrich). Cells were scraped and removed from the top of chamber. Membranes were mounted on cover slides, and cells were counted. The cell migration was quantified by counting the amount of cells passing through the pores from five different fields per sample at 100× selected in a random manner. For invasion assays, matrigel (BD Biosciences, San Jose CA, USA) diluted to 1 mg/ml in serum free-cold cell culture media was added in the top of an 8.0-μm-pore membrane chamber (Corning Costar Corp.) and incubated at 37 °C for 4 h until the matrigel solidified. Cells (0.5×10^6 cells/ml) were seeded on the top chamber with matrigel-coated membrane. After 24 h of incubation, cells that had invaded to the lower chamber were fixed and stained with hematoxylin and eosin (Sigma-Aldrich). Cells were scraped and removed from the top of chamber. Membranes were mounted on cover slides, and cells were counted. The cell invasion was quantified by counting the amount of cells passing through the membrane from five different fields per sample at 100× selected in a random manner.

3.4. Construction of luciferase reporter plasmids and dual-luciferase activity assay

The leukemia inhibitory factor receptor (*Lifr*) 3′-UTR sequences were amplified by PCR using the primers as follow: Forward/SpeI: 5′-GGACTAGTCAGTGTCACCGTGTCACTTCAG-3′; Reverse/PstI: 5′-AACTGCAGACTTGGACATTTTCTCCCTGGC-3′. After being double digested with *Spe* I and *Pst* I, the PCR product was cloned into the

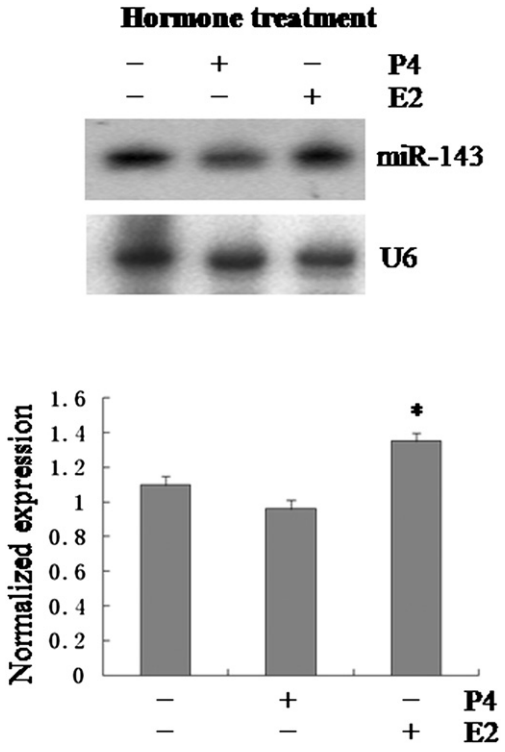

Fig. 5. The effect of steroid hormone on *miR-143* expression analyzed by Northern blot. *U6* snRNA was used as loading control to normalize for gel loading and transfer. The experiment was repeated three times. $^{*}P < 0.05$.

downstream of the firefly luciferase gene in pGL3 control vector (Promega). Deleting *miR-143* target sites in the 3′-UTR of *Lifr* was used as negative control. All these constructs were verified by DNA sequencing.

For luciferase reporter assays, ESCs or 293 T cells were seeded in 48-well plates and allowed to attach overnight, then transfected with 50 nM of the miRNA mimics, miRNA inhibitor, pre-miR control or anti-miR control (GenePharma Co.,Ltd, Shanghai, China) by using lipofectamine 2000 (Invitrogen). HEC-1B cells were also transfected with wild-type or mutant reporter plasmid. pRL-TK containing Renilla luciferase was co-transfected for data normalization. Two days later, cells were harvested and the luciferase activity was measured with the dual-luciferase assay (Promega). Each treatment was performed in triplicate in three independent experiments. The results were expressed as relative luciferase activity (Firefly LUC/Renilla LUC).

3.5. Western blot

Cell protein lysates were boiled in SDS/β-mercaptoethanol sample buffer, and 60 μg samples were loaded into each lane of 12% polyacrylamide gels. The proteins were separated by electrophoresis and transferred to polyvinylidene fluoride membrane (PVDF) (Amersham Pharmacia Biotech) by electrophoretic transfer. The membrane was incubated with rabbit anti-LIFR (No. sc-519; Santa Cruz Biotechnology Inc., Santa Cruz, CA, USA) or mo anti-β-ACTIN polyclonal antibody (No. sc-1616-R; Santa Cruz Biotechnology Inc.) diluted to 1:500 in TBST (10 mM Tris, pH 7.5, and 150 mM NaCl, pH 7.4, 0.1% Tween-20) overnight at 4 °C. The specific protein–antibody complex was detected by using horseradish peroxidase (HRP) conjugated goat anti-rabbit IgG (Jackson Immunoresearch Laboratories, West Grove, PA, USA). Detection by the chemiluminescence reaction was executed using the ECL kit (Millipore, Billerica, MA, USA). The β-ACTIN signal was used as a loading control. The experiment was repeated at least three times. The bands were analyzed using Quantity One analyzing system (Bio-Rad).

3.6. Immunohistochemistry

Sections (4 μm) of uterine tissues were deparaffinized in xylene and rehydrated in descending ethanol series. Antigen retrieval was accomplished through microwave irradiation of the sections in 10 mM sodium citrate buffer. Sections were blocked with normal goat serum for 20 min, and then incubated with rabbit anti-LIFR (No. sc-519; Santa Cruz Biotechnology Inc.) diluted to 1:200 in phosphate-buffered saline (PBS) at 4 °C overnight. Sections were treated with hydrogen peroxide (0.3% in methanol) for 10 min at room temperature to eliminate endogenous peroxidase, and then incubated with horseradish peroxidase (HRP)-conjugated goat anti-rabbit IgG (Jackson Immunoresearch Laboratories) at 37 °C for 1 h. The antibody stains were developed by addition of diaminobenzidine (DAB; Sigma-Aldrich) and cell nuclei were stained with hematoxylin (Sigma-Aldrich). To evaluate the specificity of the antibodies, negative control was performed by replacing the primary antibodies with normal goat serum. Samples were viewed using under Nikon TE 2000-U microscope (NIKON).

3.7. Statistical analysis

There are at least three rats in each treatment group. The results of Northern blot and *in situ* hybridization were repeated three times. All values are reported as the mean ± SE. Statistical analysis was done using one-way ANOVA. When significant effects of treatments were indicated, the Student–Newman–Keuls multi-range test was applied using SPSS version 13.0 (SPSS Inc., Chicago, IL, USA). $P < 0.05$ was considered statistically significant.

4. Results

4.1. Enhanced expression of miR-143 in rat uterus during early pregnancy

In this study, we first examined the expression pattern of *miR-143* in rat uterus during the peri-implantation period. Northern blot results showed that the expression level of *miR-143* on g.d. 5–8 was higher than on g.d. 3–4 ($P < 0.05$; Fig. 1A). The expression of *miR-143* in the endometrium between the implantation sites and the inter-implantation sites on day 6 of pregnancy was detected by TaqMan miRNA RT-Real Time PCR. The *miR-143* level was slightly lower in the inter-implantation sites than that in the implantation sites, but not statistical significance (Fig. 1B). *In situ* hybridization results showed that *miR-143* was mainly located in the glandular and luminal epithelia on g.d. 3 (Fig. 1 C*a*) and also appeared in the superficial stroma on g.d. 4 (Fig. 1 C*b*). On g.d. 5, positive signals of *miR-143* were strengthened in the luminal epithelia and superficial stroma (Fig. 1 C*c*). On g.d. 6, strong staining of *miR-143* in the inter-implantation sites was found in the glandular and luminal epithelia and decidua basalis (Fig. 1 C*d*). In the implantation sites, strong signals of *miR-143* were detected in the luminal epithelia and primary decidual zone (Fig. 1 C*e*). On g.d. 7, staining of *miR-143* in the inter-implantation sites was strong in the decidua basalis (Fig. 1 C*f*). In the implantation sites, the intensive staining of *miR-143* was observed in the secondary decidual zone (Fig. 1 C*g*). The intensity of *miR-143* staining was not observably different between the inter-implantation sites and the implantation sites.

4.2. MiR-143 expression was regulated by activation of delayed implantation and artificial decidualization

To detect the effect of embryonic and uterine status on the expression of *miR-143* we made the models of pseudopregnancy, activation of delayed implantation and artificial decidualization.

The model of pseudopregnancy was induced by caging adult females with vasectomized males, so there was not embryo in the uterus of the female rat of pseudopregnancy. The level of *miR-143* in uteri from the day 3–4 of pseudopregnancy was similar with that on day 5–7 (Fig. 2).

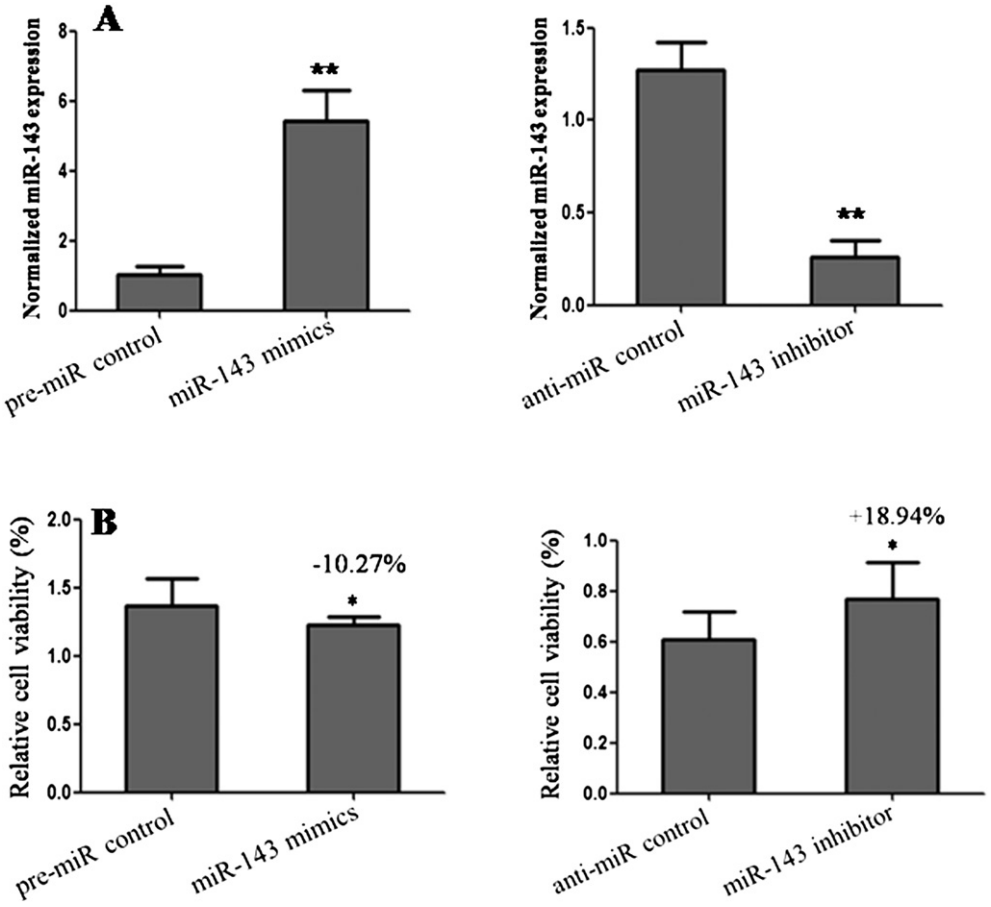

Fig. 6. MTS assay detected the effect of *miR-143* on proliferation. ESCs cells were respectively seeded in 96-well and 24-well plates, and then transfected with *miR-143* mimics, pre-miR control, *miR-143* inhibitor or anti-miR control. Two days later, cells in 24-well plates were used to detect *miR-143* expression by TaqMan miRNA RT-real time PCR (A). U6 serves as an internal reference. Cells in 96-well plates were treated with MTT and further incubated for 4 h. Absorbance was recorded at A570 nm with a 96-well plate reader (Bio-Rad 3550). $^{*}P < 0.05$; $^{**}P < 0.01$.

The above-mentioned study showed that the expression level of *miR-143* on g.d. 5–7 was higher than on g.d. 3–4 on normal pregnancy. Rat embryos enter uterus at day 3 of pregnancy and remain in a state of dormancy on day 4.5 of pregnancy until the endometrium enters receptive state on day 5, then embryo implantation is initiated on day 5.5 [20,33]. The results from pseudopregnant rats imply that *miR-143* expression was not dependent upon the presence of dormant embryos.

The ovariectomized pregnant rats are injected with progesterone to maintain delayed implantation and the blastocysts are dormant. The delayed-implantation rats are treated with estradiol-17β to terminate delayed implantation and activate the blastocysts. Low levels of *miR-143* were found in the uterus under delayed implantation condition, but *miR-143* levels were significantly enhanced after implantation was activated with estrogen treatment ($P < 0.05$; Fig. 3A), suggesting that *miR-143* expression was dependent upon activated blastocysts, not dormant blastocysts. In the model of delayed implantation, weak *miR-143* staining was found in the luminal epithelia (Fig. 3B *a*) and stroma (Fig. 3B *b*). After delayed implantation was terminated by estrogen treatment and embryos began to implant, strong *miR-143* signals were detected in the decidual zone (Fig. 3B *c*).

The model of artificial decidualization was induced by infusing olive oil into the lumen of one of the uterine horns. The contralateral uterine horn was served as a control. The expression levels of *miR-143* in the decidualized uterus were higher than that in the control uterus ($P < 0.05$; Fig. 4A). *In situ* hybridization results showed that weak signals of *miR-143* were found in the stroma, glandular and luminal epithelia in the control uterine horn (Fig. 4B *a*). However, in the decidualized uterus, strong stainings were observed in the decidual zone, glandular and luminal epithelia (Fig. 4B *b*).

4.3. Estradiol-17β promotes the expression of miR-143

The effects of steroid hormones on *miR-143* expression were examined by Northern blot (Fig. 5). Progesterone treatment slightly decreased the expression of *miR-143*. Treatment with estradiol-17β significantly enhanced the expression of *miR-143* ($P < 0.05$).

4.4. Up-regulation of miR-143 inhibits the cell proliferation

To assess the possible function of *miR-143* in the process of embryo implantation, the effect of *miR-143* on the growth of endometrial stromal cells was detected using *in vitro* cell lines model. Firstly, the effect of *miR-143* mimic and inhibitor on the expression level of *miR-143* in endometrial stromal cells was detected by TaqMan miRNA RT-Real Time PCR. The results showed that *miR-143* expression level was significantly enhanced in cells transfected with *miR-143* mimic compared with pre-miR control ($P < 0.01$), and markedly decreased in cells transfected with *miR-143* inhibitor compared with pre-miR control ($P < 0.01$) (Fig. 6A). Hereafter, cell proliferation and viability were measured by MTS assay Cell-Light Edu Apollo DNA *in vitro* kit (Fig. 6B). The relative proliferation rates in ESCs transfected with *miR-143* mimics were diminished approximately 10.27% compared with pre-miR control ($P < 0.05$). The relative

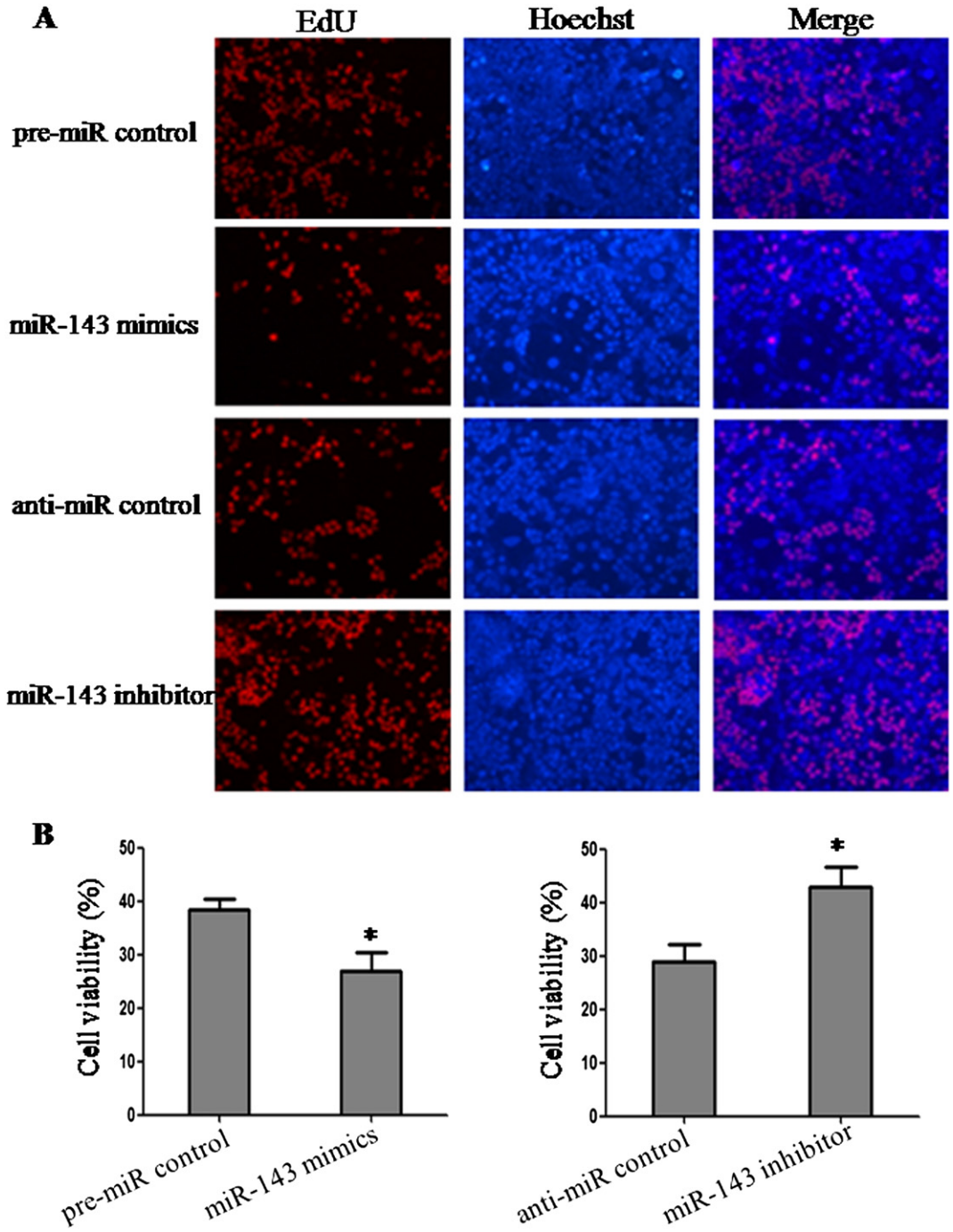

Fig. 7. The effect of *miR-143* on proliferation detected by Cell-Light Edu Apollo DNA *in vitro* Kit. ESC cells were transfected with the *miR-143* mimics, pre-miR control, *miR-143* inhibitor, or anti-miR control, respectively. Two days later, cells were treated with Cell-Light Edu and Hoechst stained nuclei (A). Red represents the proliferative cells. Blue indicates cell nuclei. The photographs were shown at ×100 original magnification. The black histogram represents the ratio of percentage of cell viability and was expressed as ratio of Edu-positive cells vs total cells (B). $^{*}p < 0.05$.

proliferation rates in cells transfected with *miR-143* inhibitor were enhanced approximately 18.94% ($P < 0.05$).

In order to further confirm the role of *miR-143* in cell viability, the proliferation capacity of U343 cells was determined by Cell-Light Edu Apollo DNA *in vitro* kit (Fig. 7). The results showed that the cell viability in ESCs transfected with *miR-143* mimics was significantly decreased compared with pre-miR control. ($P < 0.05$). While the viability of ESCs was markedly increased after transfection with *miR-143* inhibitor compared with the anti-miR control ($P < 0.05$).

Bref, these results show that over-expression of *miR-143* inhibits cell proliferation, while low-expression of *miR-143* promotes cell viability.

4.5. MiR-143 regulates migration and invasion capacity of ESCs in vitro

In order to further research the role of *miR-143* in controlling cell behavior, we analyzed the effects of *miR-143* on cell migration and invasion (Figs. 8 and 9). The results showed that the migratory capacity in ESCs transfected with *miR-143* mimics was significantly lower than that transfected with pre-miR control ($P < 0.05$). The migration capacity had an increased trend in cells transfected with *miR-143* inhibitor compared with anti-miR control (Fig. 8). Additionally, the invasion assay indicated that the invasive capacity in cells transfected with *miR-143* mimics was significantly inhibited compared with pre-miR control

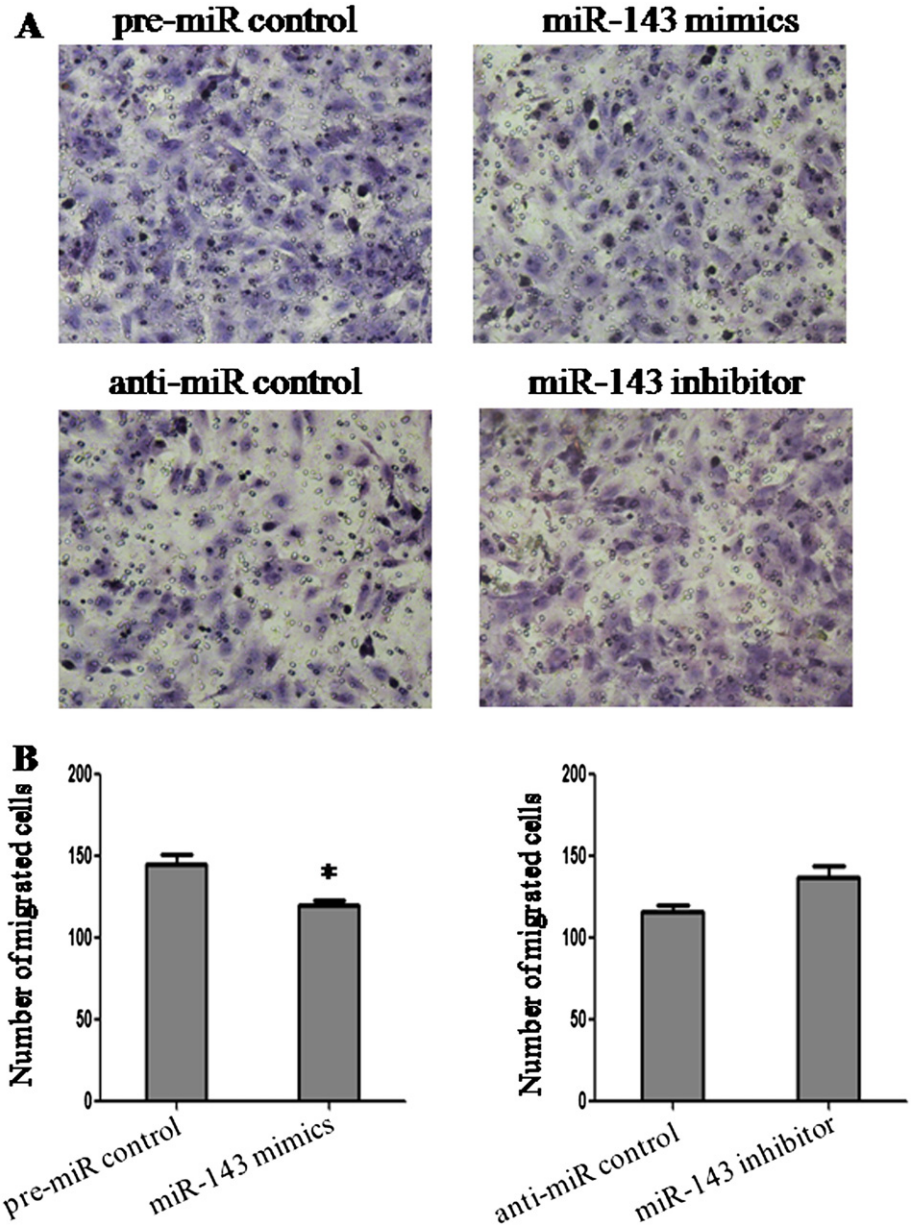

Fig. 8. The effect of *miR-143* on cell migration. ESCs were transfected with pre-miR control, *miR-143* mimics, anti-miR control or *miR-143* inhibitor, respectively. Cells were harvested 48 h after transfection and recounted to 0.5×10^6 cells/ml in every group to seed Transwells for cell migration assay. At time of harvest, the cells on top of the membranes were removed, and the cells on the bottoms of the membranes were stained with hematoxylin and eosin (A). The cell migration was quantified by counting the amount of cells passing through the membrane from five different fields per sample at 200× selected in a random manner (B).

($P < 0.05$). While cells were transfected with *miR-143* inhibitor, the invasive ability was obviously enhanced compared with anti-miR control (($P < 0.05$; Fig. 9). These findings show that the high level of *miR-143* can suppress cell invasion, implying that the high expression of *miR-143* in implantation period may contribute to prevent excessive invasion of uterine tissue by trophoblast.

4.6. Lifr is the target gene of miR-143

Because miRNAs elicit their functions by binding to the 3′ untranslated region (3′UTR) of their target mRNAs (1–3, [11,12,38]), we search *miR-143* targets by TargetScan databases (http://genes.mit.edu/targetscan.test/ucsc.html) and PicTar (http://pictar.mdc-berlin.de/) and found that there was one conservative *miR-143* responsive element in 3′-UTR of *Lifr* (Fig. 10A).

To validate *Lifr* as the target of *miR-143*, we set up a luciferase reporter assay. The 3′-UTR fragment of wild-type *Lifr* of rat containing the binding sites of *miR-143* was cloned into the downstream of the firefly luciferase reporter gene in the pGL3 control vector (designated as LIFR-pGL3) for the dual-luciferase assay (Fig. 10B). LIFR-pGL3 was co-transfected with *miR-143* mimics or inhibitor (Fig. 10C, D). Compared with the pre-miR control, the luciferase activity in ESCs and 293 T cells co-transfected with *miR-143* mimics and LIFR-pGL3 was decreased about 28.95% and 20.09%, respectively ($P < 0.01$). Furthermore, the luciferase activity was up-regulated about 33.06% and 27.28% in cells co-transfected with *miR-143* inhibitor and LIFR-pGL3, respectively, compared with the anti-miR control ($P < 0.01$). These results indicate that *miR-143* dysregulation affects the binding capacity of *miR-143* and 3′-UTR of *Lifr*, leading to the alteration of *Lifr* translation.

Base mutation of seed region was also performed to further confirm the binding site for *miR-143* in the 3′-UTR of *Lifr* (Fig. 10C, D). Mutating the putative *miR-143* binding region in the 3′-UTR of *Lifr* (designated as LIFR-pGL3-mut) was used as control. The luciferase activity was decreased about 48.19% and 44.94% in cells co-

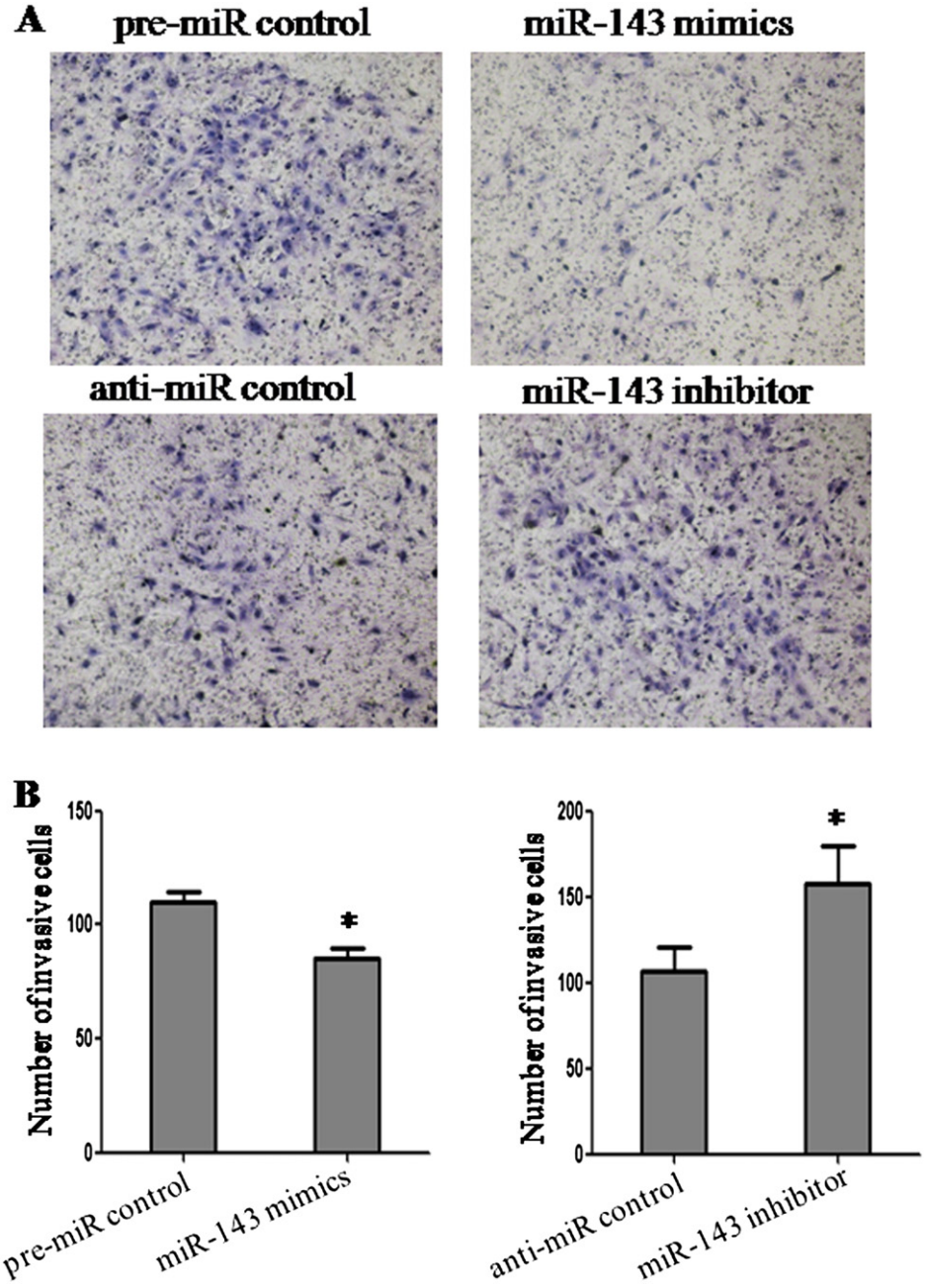

Fig. 9. The effect of *miR-143* on cell invasion. ESCs were transfected with pre-miR control, *miR-143* mimics, anti-miR control or *miR-143* inhibitor, respectively. Cells were harvested 48 h after transfection and recounted to 0.5×10^6 cells/ml in every group to seed matrigel-coated Transwells for cell invasion assay. At time of harvest, the cells on top of the membranes were removed, and the cells on the bottoms of the membranes were stained with hematoxylin and eosin (A). The cell invasion was quantified by counting the amount of cells passing through the membrane from five different fields per sample at 200× selected in a random manner (B).

transfected with *miR-143* mimics and LIFR-pGL3, respectively, compared with LIFR-pGL3-mut ($P < 0.01$). These data indicate that *miR-143* may restrain target gene expression through binding to seed sequence in the 3′-UTR of *Lifr*.

4.7. MiR-143 regulats LIFR expression in vitro

To ascertain the effect of *miR-143* on LIFR expression, we transfected 293 T cells with *miR-143* mimics or inhibitor to detect the change of LIFR protein level (Fig. 11). Compared with pre-miR control, LIFR protein levels were significantly decreased by *miR-143* mimics ($P < 0.05$). Additionally, compared with anti-miR control, LIFR protein levels in 293 T cells were measurably increased by the *miR-143* inhibitor ($P < 0.05$).

4.8. Localization of LIFR in rat uterus

Localization of LIFR in rat uterus during early pregnancy was detected by immunohistochemistry (Fig. 12). Strong intensity of LIFR staining was observed in the glandular and luminal epithelia and superficial stroma on g.d. 3 and 4 (Fig. 12A and B). On g.d. 5, positive signals of LIFR were weakened in the glandular and luminal epithelia and superficial stroma (Fig. 12C). On g.d. 6 and 7, staining of LIFR in the inter-implantation sites was weak and mainly located in the decidua basalis (Fig. 12D and F). In the implantation sites, positive signals of LIFR

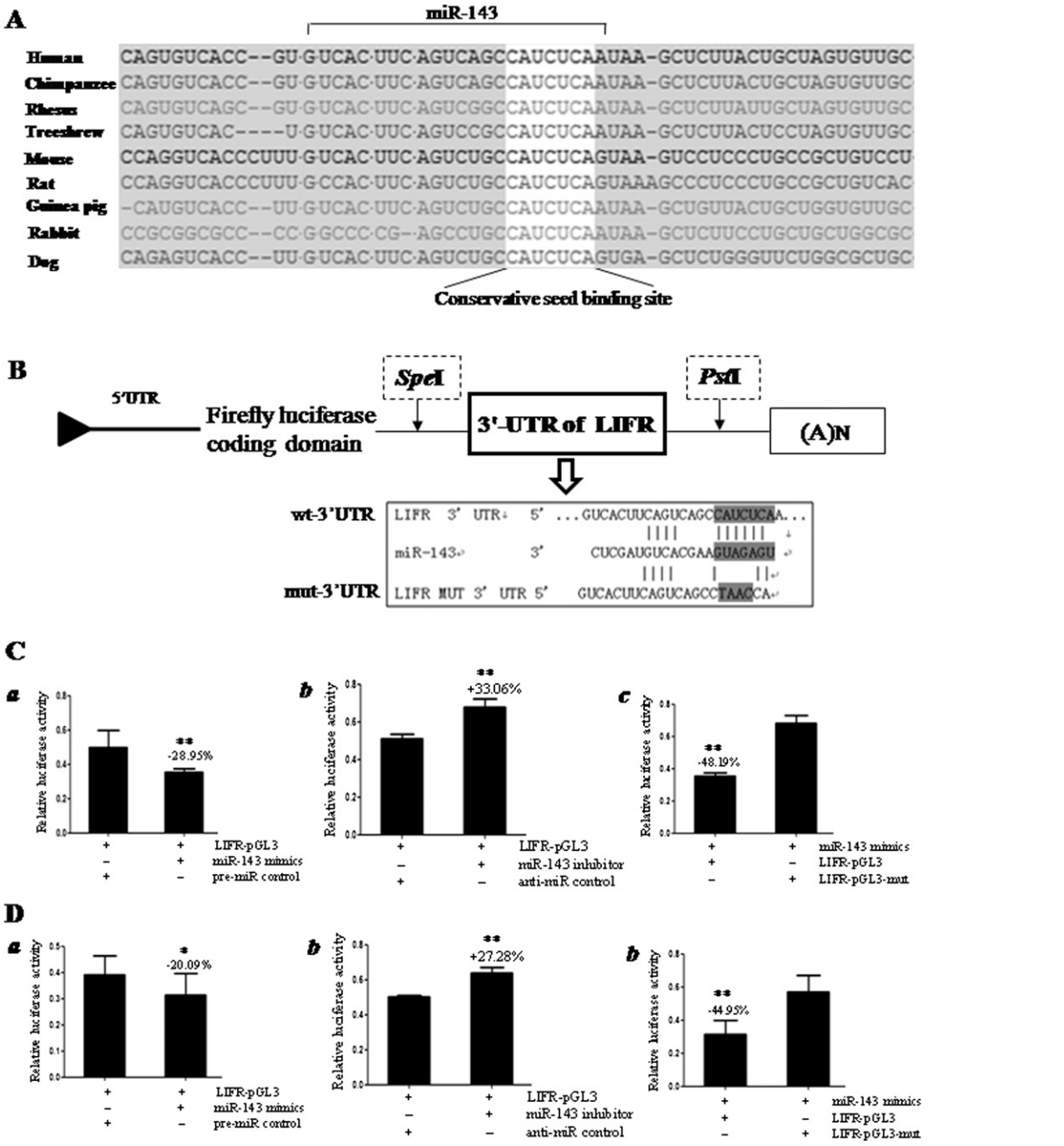

Fig. 10. The prediction and confirmation of the *miR-143* target gene. *MiR-143* binding sites in the 3′-UTR region of *Lifr* was compared in cross-species (A). The 3′-UTR fragment of wild-type *Lifr* of rat containing the binding sites of *miR-143* was cloned into the downstream of the firefly luciferase reporter gene in the pGL3 control vector (designated as pGL3-Lifr) for the dual-luciferase assay (B). ESCs (C) and 293 T cells (D) were co-transfected with *miR-143* mimics, pre-miR control (C *a* and D *a*), *miR-143* inhibitor, or anti-miR control (C *b* and D *b*), and pGL3-Lifr for dual-luciferase assay. Deleting putative *miR-143* binding region in the 3′-UTR of *Lifr* (designated as pGL3-Lifr-mut) was used as control (C *c* and D *c*). pRL-TK containing Renilla luciferase was co-transfected for data normalization. $^{*}P < 0.05$, $^{**}P < 0.01$.

were also weak and mainly observed in the primary decidual zone on g.d. 6 and the secondary decidual zone on g.d. 7 (Fig. 12E and G). The intensity of LIFR staining was not visibly different between the inter-implantation sites and the implantation sites. In the model of delayed implantation, strong LIFR staining was found in the stroma (Fig. 12H and I). After delayed implantation was terminated by estrogen treatment and embryos began to implant, weak LIFR signals were observed in the decidua basalis (Fig. 12J). In the model of artificial decidualization, strong LIFR signals were found in the stroma in the control uterine horn (Fig. 12K). However, in the decidualized uterus, weak staining was detected in the decidual zone (Fig. 12L).

5. Discussion

Our previous study showed that *miR-143* was differentially expressed in rat uteri between pre-receptive and receptive phase via microRNA (miRNA) microarray analysis [40]. However, the expression pattern and function of *miR-143* during embryo implantation in rat remain unknown. To study the role of *miR-143* in embryo implantation, we first examined its spatialtemporal distribution in rat uterus during the peri-implantation period. The expression of uterine *miR-143* on g.d. 5–8 was higher than that on g.d. 3–4, and it mainly located in the glandular and luminal epithelia, stroma or decidua. Hu et al [15] had

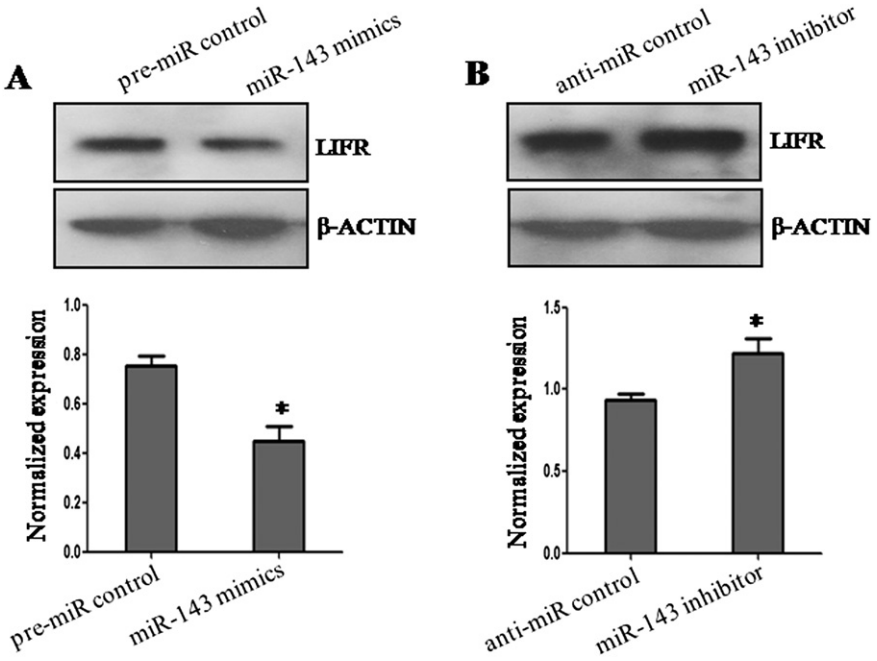

Fig. 11. The effect of *miR-143* on endogenous LIFR expression. LIFR protein levels in *miR-143* mimics (A) and inhibitor (B)-treated HEC-1B cells were detected by Western blot. Total protein was separated by SDS-PAGE, then transferred to PVDF membrane. The membrane was incubated with LIFR or β-ACTIN antibody and detected by the enhanced chemiluminescence (ECL) detection system. The histogram represents the optical densities of the signals quantified by densitometric analysis and represented as LIFR intensity/β-ACTIN intensity to normalize for gel loading and transfer. $^{*}P < 0.05$.

reported that *miR-143* was up-regulated at least 2-fold at implantation sites in the mouse uterus on day 5 of pregnancy compared with inter-implantation sites. Embryonic preparation for implantation needs the initiation of blastocyst activation and uterine receptivity [32,46,47]. In rat, the endometrium becomes receptive on day 5, then embryo implantation can be initiated on day 5.5 [20,33]. After onset of embryo implantation, the underlying endometrial stromal cells undergo decidualization [33] and an increase of *miR-143* expression in the stroma during the receptive phase may contribute to stromal-decidual transformation. These facts suggested that the *miR-143* may play a crucial role in embryo implantation and be involved in the endometrial receptivity or endometrial decidualization.

In order to further research the relationship between *miR-143* and embryo implantation, we utilized the model of pseudopregnancy,

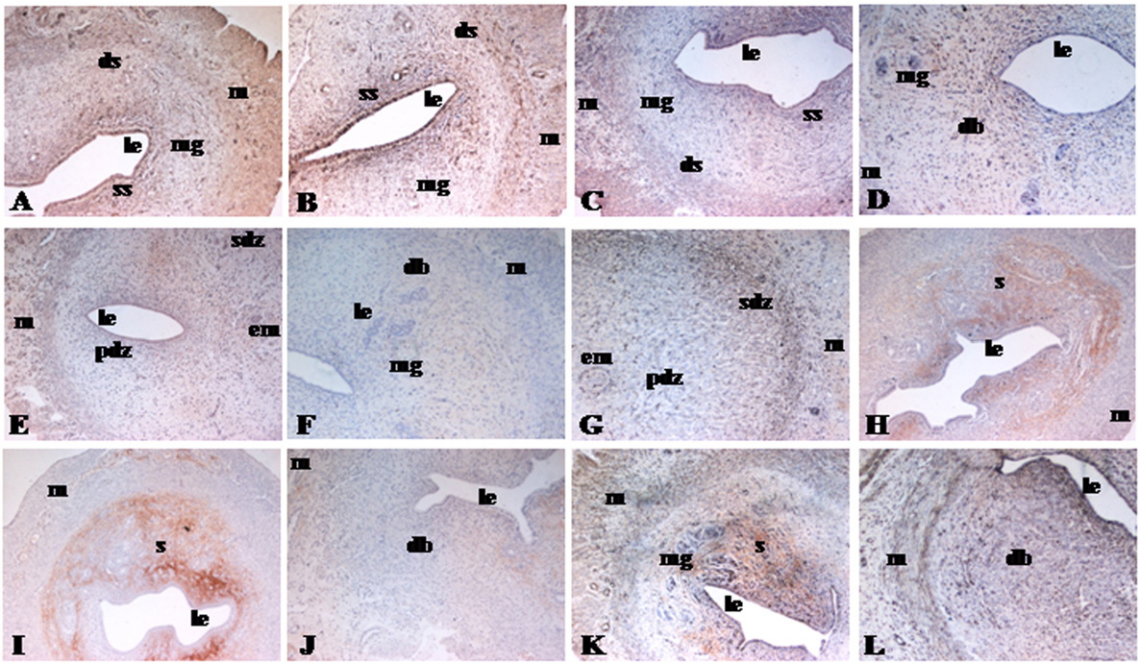

Fig. 12. The expression of LIFR in rat uteri. Localization of LIFR in rat uteri from day 3 (A), day 4 (B), day 5(C), inter-implantation sites and implantation sites of day 6 (D and E) and day 7 (F and G) of pregnancy, the delayed implantation (H and I) and activation of delayed implantation (J), the non-stimulated (K) and stimulated (L) of artificial decidualization were measured by immunohistochemistry using LIFR antibody. The sections were incubated with normal goat serum as negative control (not shown). The staining was developed with DAB and the nuclei were stained with hematoxylin. The photographs are shown at ×100 original magnification. Key: m, myometrium; mg, maternal gland; le, luminal epithelium; ss, superficial stroma; ds, deep stroma; pdz, primary decidual zone; sdz, secondary decidual zone; s, stroma; db, decidua basalis; em, embryo.

activation of delayed implantation and artificial decidualization to analyze the change in *miR-143* level. The results showed that *miR-143* levels were similar in rat uteri from day 3 to 7 of pseudopregnancy. In the model of activation of delayed implantation, the expression of *miR-143* was low under delayed implantation conditions, but it significantly increased after activation of delayed implantation with estrogen treatment. In the model of artificial decidualization, the expression levels of *miR-143* in the decidualized uterus were significantly enhanced. A female rat was mated with a vasectomized male rat to obtain a pseudopregnant rat, so there were not embryos in uteri of pseudopregnant rat [17,28]. Blastocysts were activated and embryos implantation was initiated by estrogen treatment in the model of activation of delayed implantation [26,35]. Decidualization was artificially induced by infusing olive oil into the lumen of uteri of pseudopregnant rats [8]. A comprehensive analysis of the characteristics of these models and *miR-143* expression pattern implies that the increase of *miR-143* expression is dependent on blastocyst activation and decidualization.

In this study, we also examine the influence of steroid hormones on miRNA expression under simulative physiological conditions. We found that estradiol-17β observably promoted the expression of *miR-143* in the ovariectomized rat uterus. Estrogen is a critical determinant that specifies the duration of the window of uterine receptivity for implantation [24], implying that up-regulation of *miR-143* induced by estrogen may be conducive to the open of endometrium implantation window. However, the expression of *miR-143* was repressed by E2 in breast cancer cells [2]. Although embryo implantation shares the similar phenomena and mechanisms with tumor development [29], the functions of E2 are different between embryo implantation and carcinogenesis [24,41], which may be partial reasons that the expression trend of *miR-143* mediated by E2 is inverse between the ovariectomized rat uterus and breast cancer cells. E2 is essential for embryo implantation in rat and mouse [6,16]. The up-regulation of *miR-143* induced by E2 in uterus of ovariectomized rat implies that miR-143 may be involved in early pregnancy events.

To explore the possible role of *miR-143* in embryo implantation, we tested the effect of *miR-143* on cell growth, migration and invasion. Gain of function of *miR-143* in ESCs inhibited cell proliferation, migration and invasion. Loss of function of *miR-143* accelerated cell proliferation and invasion. The phenomenon was consistent with the reports of Zhang et al. [48], Wu et al. [39] and Qian et al. [34] that *miR-143* inhibited growth and migration and induced apoptosis in human leukemia, gastric and colorectal cancers cells. In addition, after onset of embryo implantation, uterine stromal cell decidualization begins with extensive stromal cell proliferation around the site of embryo implantation and forms the primary decidual zone [25]. The stromal cells next to the primary decidual zone form the secondary decidual zone by continuing to proliferate and differentiate into polyploid decidual cells [37]. Some studies have shown that the development of decidual cell polyploidy pivotally determines proper control of uterine decidualization and early embryo implantation in mice [14,27]. Our study indicates that strong signals of *miR-143* were found in the secondary decidual zone in the implantation sites of uteri on day 7 of pregnancy in rat. Previous study has been shown that uterine decidual polyploid cells specifically lack apoptosis [42]. High level of *miR-143* in the secondary decidual zone may prevent the excessive invasion of uterine decidual polyploid cells. Therefore, the up-regulation of *miR-143* in rat uteri during implantation phase may contribute to uterine reconstruction to establish a healthy pregnancy.

It is generally accepted that miRNAs exert their roles through controlling the expression of their downstream target genes. An online search of *miR-143* targets by TargetScan and PicTar showed that there was one conservative *miR-143* responsive element in 3′-UTR of *Lifr*. The results from dual-luciferase activity and western blot assay indicated that overexpression of *miR-143* enhanced the binding capacity of *miR-143* and 3′-UTR of *Lifr*, leading to the suppression of *Lifr* translation. However, knockdown of *miR-143* diminished the binding capacity of *miR-143* and 3′-UTR of *Lifr*, leading to the strengthenment of *Lifr* translation. Additionally, in this study, base mutation of seed region in the 3′-UTR of *Lifr* was performed to further confirm the binding site between *miR-143* and its target gene. The luciferase activity was markedly decreased in cells co-transfected with *miR-143* mimics and LIFR-pGL3 compared with LIFR-pGL3-mut. These data indicate that the binding site in the 3′-UTR of *Lifr* was specific for *miR-143*. It is important for target recognition to have approximately 7 nt sites that match the seed region of the miRNA [4,7]. However, a canonical 7–8mer site is often not sufficient for detectable downregulation of target genes [10]. MiRNAs target recognition also needs five general features of site context that augment site efficacy: AU-rich nucleotide composition near the site, proximity to sites for co-expressed miRNAs, proximity to residues pairing to miRNA nucleotides 13–16, positioning within the 3′UTR at least 15 nt from the stop codon, and positioning away from the center of long UTRs [10]. Here, 7 nt sites in the 3′-UTR of *Lifr* that match the seed region of the *miR-143* have a locally AU-rich context, over 15 nt from the stop codon and near the front ends of long UTRs. Although 3′ pairing at the 3′ core (positions 13–16) being more important for efficacy than pairing to other positions, pairing started at miRNA positions 12, 13, or 14 was more evolutionarily conserved shown by Watson-Crick pairing to four contiguous miRNA nucleotides [10]. The 3′ pairing between the 3′-UTR of *Lifr* and *miR-143* has a binding region at miRNA nucleotides 12–15. All these characteristics in 3′-UTR of *Lifr* may synergistically induce the effective repression of *miR-143* target.

In this study, we detected the expression of LIFR in rat uterus during early pregnancy by immunohistochemistry. The positive signals of LIFR were observed in the glandular and luminal epithelia and superficial stroma on g.d. 3 and 4. The intensity of LIFR staining in rat uterus was weaker on g.d. 5–7 than g.d. 3–4. In the model of delayed implantation and artificial decidualization, signal strength of LIFR in uteri of activation of delayed implantation or artificial decidualization was weaker than the corresponding control. In mouse, *Lifr* mRNA was detected in the luminal epithelium on day 3 of pregnancy followed by more intense signals on day 4. Following implantation on day 5, *Lifr* mRNA was highly expressed in the luminal and glandular epithelia. [31,36]. The difference of *Lifr* expression patterns may be due to the distinction of species and gene product. In our study, the protein level of LIFR was detected by immunohistochemistry. In the studies of Song and Lim and Ni et al., the mRNA level of *Lifr* was detected by *in situ* hybridization. We found that the tendency between the intensity of *miR-143* staining and the intensity of LIFR staining is opposite in rat uteri during early pregnancy. Additionally, the intensity of LIFR or *miR-143* staining was not visibly different between the inter-implantation sites and the implantation sites. All these facts imply that *miR-143* expression may be inversely correlated with LIFR expression during early pregnancy in rat.

These data confirm that *Lifr* is the target gene of *miR-143*. Leukemia inhibitory factor (Lif) exerts its effects by binding to *Lifr* [3,5]. Lif facilitates the development of ectopic pregnancy by stimulating blastocyst adhesion and trophoblast outgrowth from placental explants [23]. Therefore, the up-regulation of *miR-143* in implantation period may contribute to inhibit the excessive outgrowth of trophoblastic cells by adjusting *Lifr*.

6. Conclusions

The enhancement of *miR-143* level in rat uterus during implantation phase is associated with blastocysts activation and uterine decidualization. Enforced *miR-143* expression inhibits cell proliferation and invasion, which may partly through repressing *Lifr*.

Funding

This work was funded by grants from the Natural Science Foundation of China (No. 81370720). We are particularly grateful to the National Research Institute for Family Planning (No. 2012GJSSJKA03) for its help in fund and equipment.

References

[1] K. Banno, M. Iida, M. Yanokura, I. Kisu, T. Iwata, E. Tominaga, K. Tanaka, D. Aoki, MicroRNA in cervical cancer: OncomiRs and tumor suppressor miRs in diagnosis and treatment, ScientificWorldJournal 2014 (2014) 178075.

[2] P. Bhat-Nakshatri, G. Wang, N.R. Collins, M.J. Thomson, T.R. Geistlinger, J.S. Carroll, M. Brown, S. Hammond, E.F. Srour, Y. Liu, H. Nakshatri, Estradiol-regulated microRNAs control estradiol response in breast cancer cells, Nucleic Acids Res. 37 (2009) 4850–4861.

[3] F. Blanchard, L. Duplomb, Y. Wang, O. Robledo, E. Kinzie, V. Pitard, A. Godard, Y. Jacques, H. Baumann, Stimulation of leukemia inhibitory factor receptor degradation by extracellular signal-regulated kinase, J. Biol. Chem. 275 (2000) 28793–28801.

[4] J. Brennecke, A. Stark, R.B. Russell, S.M. Cohen, Principles of microRNA-target recognition, PLoS Biol. 3 (2005) e85.

[5] A.P. Catunda, E. Gócza, B.V. Carstea, L. Hiripi, H. Hayes, C. Rogel-Gaillard, M. Bertaud, Z. Bosze, Characterization, chromosomal assignment, and role of LIFR in early embryogenesis and stem cell establishment of rabbits, Cloning Stem Cells 10 (2008) 523–534.

[6] S.K. Dey, D.C. Johnson, P.L. Pakrasi, J.G. Liehr, Estrogens with reduced catechol-forming capacity fail to induce implantation in the rat, Proc. Soc. Exp. Biol. Med. 181 (1986) 215–218.

[7] J.G. Doench, P.A. Sharp, Specificity of microRNA target selection in translational repression, Genes Dev. 18 (2004) 504–511.

[8] C.A. Finn, P.M. Keen, The induction of deciduomata in the rat, J. Embryol. Exp. Morpholog. 11 (1963) 673–682.

[9] C.M. Gits, P.F. van Kuijk, M.B. Jonkers, A.W. Boersma, M. Smid, W.F. van Ijcken, J.M. Coindre, F. Chibon, C. Verhoef, R.H. Mathijssen, M.A. den Bakker, J. Verweij, S. Sleijfer, E.A. Wiemer, MicroRNA expression profiles distinguish liposarcoma subtypes and implicate miR-145 and miR-451 as tumor suppressors, Int. J. Cancer 135 (2014) 348–361.

[10] A. Grimson, K.K. Farh, W.K. Johnston, P. Garrett-Engele, L.P. Lim, D.P. Bartel, MicroRNA targeting specificity in mammals: determinants beyond seed pairing, Mol. Cell 27 (2007) 91–105.

[11] Y. Guo, L. Ying, Y. Tian, P. Yang, Y. Zhu, Z. Wang, F. Qiu, J. Lin, MiR-144 downregulation increases bladder cancer cell proliferation by targeting EZH2 and regulating Wnt signaling, FEBS J. 280 (2013) 4531–4538.

[12] Z.B. Han, Z. Yang, Y. Chi, L. Zhang, Y. Wang, Y. Ji, J. Wang, H. Zhao, Z.C. Han, MicroRNA-124 suppresses breast cancer cell growth and motility by targeting CD151, Cell. Physiol. Biochem. 31 (2013) 823–832.

[13] M. Hart, E. Nolte, S. Wach, J. Szczyrba, H. Taubert, T. Rau, A. Hartmann, F.A. Grasser, B. Wullich, Comparative microRNA profiling of prostate carcinomas with increasing tumor stage by deep-sequencing, Mol. Cancer Res. 12 (2014) 250–263.

[14] Y. Hirota, T. Daikoku, S. Tranguch, H. Xie, H.B. Bradshaw, S.K. Dey, Uterine-specific p53 deficiency confers premature uterine senescence and promotes preterm birth in mice, J. Clin. Invest. 120 (2010) 803–815.

[15] S.J. Hu, G. Ren, J.L. Liu, Z.A. Zhao, Y.S. Yu, R.W. Su, X.H. Ma, H. Ni, W. Lei, Z.M. Yang, MicroRNA expression and regulation in mouse uterus during embryo implantation, J. Biol. Chem. 283 (2008) 23473–23484.

[16] Y.M. Huet, S.K. Dey, Role of early and late oestrogenic effects on implantation in the mouse, J. Reprod. Fertil. 81 (1987) 453–458.

[17] H. Inano, K. Suzuki, Radiation-induced mammary tumorigenesis in pseudopregnant rats mated with vasectomized partners, Cancer Lett. 116 (1997) 241–245.

[18] T. Itesako, N. Seki, H. Yoshino, T. Chiyomaru, T. Yamasaki, H. Hidaka, T. Yonezawa, N. Nohata, T. Kinoshita, M. Nakagawa, H. Enokida, The MicroRNA expression signature of bladder cancer by deep sequencing: the functional significance of the miR-195/497 cluster, PLoS ONE 9 (2014) e84311.

[19] C. Josse, N. Bouznad, P. Geurts, A. Irrthum, V.A. Huynh-Thu, L. Servais, A. Hego, P. Delvenne, V. Bours, C. Oury, Identification of a microRNA landscape targeting the PI3K/Akt signaling pathway in inflammation-induced colorectal carcinogenesis, Am. J. Physiol. Gastrointest. Liver Physiol. 306 (2014) G229–G243.

[20] T.G. Kennedy, C. Gillio-Meina, S.H. Phang, Prostaglandins and the initiation of blastocyst implantation and decidualization, Reproduction 134 (2007) 635–643.

[21] Y. Kitade, Y. Akao, MicroRNAs and their therapeutic potential for human diseases: microRNAs, miR-143 and -145, function as anti-oncomirs and the application of chemically modified miR-143 as an anti-cancer drug, J. Pharmacol. Sci. 114 (2010) 276–280.

[22] S. Kojima, H. Enokida, H. Yoshino, T. Itesako, T. Chiyomaru, T. Kinoshita, M. Fuse, R. Nishikawa, Y. Goto, Y. Naya, M. Nakagawa, N. Seki, The tumor-suppressive microRNA-143/145 cluster inhibits cell migration and invasion by targeting GOLM1 in prostate cancer, J. Hum. Genet. 59 (2014) 78–87.

[23] T. Krishnan, A. Winship, S. Sonderegger, E. Menkhorst, A.W. Horne, J. Brown, J.G. Zhang, N.A. Nicola, S. Tong, E. Dimitriadis, The role of leukemia inhibitory factor in tubal ectopic pregnancy, Placenta 34 (2013) 1014–1019.

[24] W.G. Ma, H. Song, S.K. Das, B.C. Paria, S.K. Dey, Estrogen is a critical determinant that specifies the duration of the window of uterine receptivity for implantation, Proc. Natl. Acad. Sci. U. S. A. 100 (2003) 2963–2968.

[25] X. Ma, F. Gao, A. Rusie, J. Hemingway, A.B. Ostmann, J.M. Sroga, A.G. Jegga, S.K. Das, Decidual cell polyploidization necessitates mitochondrial activity, PLoS ONE 6 (2011) e26774.

[26] D. Martel, A. Psychoyos, Endometrial content of nuclear estrogen receptor and receptivity for ovoimplantation in the rat, Endocrinology 99 (1976) 470–475.

[27] M. Mori, M. Kitazume, R. Ose, J. Kurokawa, K. Koga, Y. Osuga, S. Arai, T. Miyazaki, Death effector domain-containing protein (DEDD) is required for uterine decidualization during early pregnancy in mice, J. Clin. Invest. 121 (2011) 318–327.

[28] T. Murata, K. Narita, T. Higuchi, Changes in uterine receptor mRNAs for oxytocin and estrogen in the pseudopregnant rat, J. Vet. Med. Sci. 70 (2008) 1253–1256.

[29] M.J. Murray, B.A. Lessey, Embryo implantation and tumor metastasis: common pathways of invasion and angiogenesis, Semin. Reprod. Endocrinol. 17 (1999) 275–290.

[30] E.K. Ng, R. Li, V.Y. Shin, J.M. Siu, E.S. Ma, A. Kwong, MicroRNA-143 is downregulated in breast cancer and regulates DNA methyltransferases 3A in breast cancer cells, Tumour Biol. 35 (2014) 2591–2598.

[31] H. Ni, N.Z. Ding, M.J. Harper, Z.M. Yang, Expression of leukemia inhibitory factor receptor and gp130 in mouse uterus during early pregnancy, Mol. Reprod. Dev. 63 (2002) 143–150.

[32] B.C. Paria, H. Song, X. Wang, P.C. Schmid, R.J. Krebsbach, H.H. Schmid, T.I. Bonner, A. Zimmer, S.K. Dey, Dysregulated cannabinoid signaling disrupts uterine receptivity for embryo implantation, J. Biol. Chem. 276 (2001) 20523–20528.

[33] A. Psychoyos, Hormonal control of ovoimplantation, Vitam. Horm. 31 (1973) 201–256.

[34] X. Qian, J. Yu, Y. Yin, J. He, L. Wang, Q. Li, L.Q. Zhang, C.Y. Li, Z.M. Shi, Q. Xu, W. Li, L.H. Lai, L.Z. Liu, B.H. Jiang, MicroRNA-143 inhibits tumor growth and angiogenesis and sensitizes chemosensitivity to oxaliplatin in colorectal cancers, Cell Cycle 12 (2013) 1385–1394.

[35] M.L. Ribeiro, C.A. Vercelli, M.S. Sordelli, M.G. Farina, M. Cervini, S. Billi, A.M. Franchi, 17beta-oestradiol and progesterone regulate anandamide synthesis in the rat uterus, Reprod. BioMed. Online 18 (2009) 209–218.

[36] H. Song, H. Lim, Evidence for heterodimeric association of leukemia inhibitory factor (LIF) receptor and gp130 in the mouse uterus for LIF signaling during blastocyst implantation, Reproduction 131 (2006) 341–349.

[37] J. Tan, S. Raja, M.K. Davis, O. Tawfik, S.K. Dey, S.K. Das, Evidence for coordinated interaction of cyclin D3 with p21 and cdk6 in directing the development of uterine stromal cell decidualization and polyploidy during implantation, Mech. Dev. 111 (2002) 99–113.

[38] N. Trakooljul, J.A. Hicks, H.C. Liu, Identification of target genes and pathways associated with chicken microRNA miR-143, Anim. Genet. 41 (2010) 357–364.

[39] X.L. Wu, B. Cheng, P.Y. Li, H.J. Huang, Q. Zhao, Z.L. Dan, D.A. Tian, P. Zhang, MicroRNA-143 suppresses gastric cancer cell growth and induces apoptosis by targeting COX-2, World J. Gastroenterol. 19 (2013) 7758–7765.

[40] H.F. Xia, X.H. Jin, Z.F. Cao, Y. Hu, X. Ma, MicroRNA expression and regulation in the uterus during embryo implantation in rat, FEBS J. 281 (2014) 1872–1891.

[41] J.D. Yager, Mechanisms of estrogen carcinogenesis: the role of E2/E1-quinone metabolites suggests new approaches to preventive intervention, Steroids (2014) (in press).

[42] L. Yue, T. Daikoku, X. Hou, M. Li, H. Wang, et al., Cyclin G1 and cyclin G2 are expressed in the periimplantation mouse uterus in a cell-specific and progesterone-dependent manner: evidence for aberrant regulation with Hoxa-10 deficiency, Endocrinology 146 (2005) 2424–2433.

[43] C. Yi, W.D. Xie, F. Li, Q. Lv, J. He, J. Wu, D. Gu, N. Xu, Y. Zhang, MiR-143 enhances adipogenic differentiation of 3 T3-L1 cells through targeting the coding region of mouse pleiotrophin, FEBS Lett. 585 (2011) 3303–3309.

[44] H. Yoshino, H. Enokida, T. Itesako, S. Kojima, T. Kinoshita, S. Tatarano, T. Chiyomaru, M. Nakagawa, N. Seki, Tumor-suppressive microRNA-143/145 cluster targets hexokinase-2 in renal cell carcinoma, Cancer Sci. 104 (2013) 1567–1574.

[45] X.L. Zeng, S.Y. Zhang, J.F. Zheng, H. Yuan, Y. Wang, Altered miR-143 and miR-150 expressions in peripheral blood mononuclear cells for diagnosis of non-small cell lung cancer, Chin. Med. J. (Engl.) 126 (2013) 4510–4516.

[46] S. Zhang, H. Lin, S. Kong, S. Wang, H. Wang, H. Wang, D.R. Armant, Physiological and molecular determinants of embryo implantation, Mol. Aspects Med. 34 (2013) 939–980.

[47] X. Zhang, Y. Dong, H. Ti, J. Zhao, Y. Wang, T. Li, B. Zhang, Down-regulation of miR-145 and miR-143 might be associated with DNA methyltransferase 3B overexpression and worse prognosis in endometrioid carcinomas, Hum. Pathol. 44 (2013) 2571–2580.

[48] Y.Y. Zhang, H.Y. Fu, D.S. Wu, H.R. Zhou, J.Z. Shen, Overexpression of microRNA-143 inhibits growth and induces apoptosis in human leukemia cells, Oncol. Rep. 31 (2014) 2035–2042.